AVALIAÇÃO DA LIMPEZA E REOXIDAÇÃO DE UM AÇO SAE 1055 MODIFICADO*

Pedro Cunha Alves[1]
Julio Aníbal Morales Pereira[2]
Vinicius Cardoso da Rocha[3]
Wagner Viana Bielefeldt[4]
Antônio Cezar Faria Vilela[5]

Resumo

A limpeza e a reoxidação de um aço SAE 1055 modificado foram avaliadas durante a sua produção em uma aciaria elétrica. Escória A no sistema óxido $CaO-SiO_2-MgO-Al2O_3-CaF_2$ (CSMA-F) e escórias B e C no sistema óxido $CaO-SiO_2-MgO-Al_2O_3$ (CSMA) foram analisadas. Duas amostras de aço foram coletadas em ambiente industrial: forno panela e barra laminada. ASPEX Explorer foi utilizado para obter informações sobre as inclusões, organizando-as por composição química, tamanho, densidade e tipo. FactSage v7.2 calculou as inclusões formadas durante a solidificação do aço, fração líquida e sólida das escórias e viscosidade da fração líquida. Após o refino secundário, o tipo mais comum de inclusão encontrada foram os aluminatos de cálcio. Na barra laminada, o espinélio foi o tipo de inclusão mais frequente, indicando um possível produto de reoxidação. Sua formação pode ser causada devido a interação com os materiais utilizados no distribuidor e molde. A redução da temperatura também favorece a formação de espinélios, como demonstrado pelo FactSage. As inclusões de espinélio foram analisadas pelo método Função de Densidade Populacional (PDF), que identificou que as corridas A1, A2, C1 e C2 apresentavam inclusões de espinélio formadas por reoxidação. Uso de escória no sistema CSMA é indicado já que eventos de reoxidação foram diminuídos nas corridas B1 e B2. No entanto, é necessária uma análise mais profunda dos materiais utilizados no distribuidor e molde para melhorar a limpeza do aço SAE 1055.

Palavras-chave: Reoxidação; Inclusões não-metálicas; Escória; FactSage.

STEEL CLEANLINESS AND REOXIDATION EVALUATION OF MODIFIED SAE 1055 STEEL

Abstract

Steel cleanliness and reoxidation of a modified SAE 1055 steel were evaluated during its production on an electric steel mill. Slag A in $CaO-SiO_2-MgO-Al_2O_3-CaF_2$ (CSMA-F) oxide system and slags B and C in $CaO-SiO_2-MgO-Al_2O_3$ (CSMA) oxide system were analyzed. Two steel samples were collected in industrial environment: ladle furnace and rolled bar. An ASPEX Explorer was used to obtain information about inclusions, organizing them by chemical composition, size, density and type. FactSage v7.2 calculated inclusions formed during steel solidification, liquid and solid fraction of slags and liquid viscosity. After secondary refining, most common type of inclusion was calcium aluminate. At rolled bar, spinel was the more frequent type of inclusion, indicating a possible reoxidation product. Their formation could be caused by interactions with tundish and mold materials. Reduction of temperature also favors formation of spinel as shown by FactSage. Spinel inclusions were analyzed by Population Density Function (PDF) method, which identified that heats A1, A2, C1 and C2 had spinel inclusions formed by reoxidation. Usage of slag in CSMA system is indicated since reoxidation was diminished in heats B1 and B2. Nevertheless, it would be necessary a deep analysis on tundish and mold materials to improve steel cleanliness of SAE 1055 steel.

Keywords: Reoxidation; Non-metallic inclusions; Slag; FactSage.

[1] *MSc Eng. Metalúrgico, pesquisador, Departamento de Metalurgia, Laboratório de Siderurgia (LaSid) – Universidade Federal do Rio Grande do Sul (UFRGS), Porto Alegre, RS, Brasil.*
[2] *Dr Eng. Metalúrgico, pesquisador, Departamento de Metalurgia, LaSid/UFRGS, Porto Alegre, RS, Brasil.*
[3] *MSc Eng. Metalúrgico, doutorando, Departamento de Metalurgia, LaSid/UFRGS, Porto Alegre, RS, Brasil.*
[4] *Professor, Dr., Departamento de Metalurgia, LaSid/UFRGS, Porto Alegre, RS, Brasil.*
[5] *Professor, Dr.-Ing., Departamento de Metalurgia, LaSid/UFRGS, Porto Alegre, RS, Brasil.*

** Contribuição técnica ao 50º Seminário de Aciaria, Fundição e Metalurgia de Não-Ferrosos, parte integrante da ABM Week 2019, realizada de 01 a 03 de outubro de 2019, São Paulo, SP, Brasil.*

1 INTRODUCTION

Steel cleanliness standards are increasing each year and inclusion control during steelmaking becomes crucial [1,2]. Previous works in the past years evaluate slag chemical composition and their relation with steel cleanliness [3-8]. Since removal of inclusions usually occurs in the ladle furnace and it is performed by slag, this information is paramount for metallurgists [4]. In general, literature provides great information regarding the production of different steel grades and the slag that match cleanliness requirements. However, before solidification process, liquid steel pass through tundish and mold in a continuous casting station. At this moment, reoxidation events can take control being harmful to steel cleanliness [9,10]. Over the past years reoxidation at this stage of the process is being evaluate, bringing new insights to improve steel cleanliness [11-13]. An active tundish slag, capable to remove inclusion during tundish metallurgy and improved chemical composition of gunning mass material are examples of industrial practices that could be adopted to diminish reoxidation [9,11].

Automated inclusion analysis surge as one of the main tools to evaluate inclusion population. This method provides information such as chemical composition, size, density and area fraction of inclusions [14-16]. With these data, it is possible to compare and evaluate reoxidation based on inclusion population for different stages of steelmaking process. Inclusions size information also can be used in Population Density Function (PDF) method to obtain more results about reoxidation [17-19]. This analysis evaluates if inclusion were formed due to reoxidation, presenting a lognormal or linear fit as output result [17]. Lognormal curve indicates that inclusions were formed by reoxidation [17]. FactSage can corroborate the results found in previous analysis mentioned providing thermodynamic equilibrium results [20]. Inclusions formed due to the different steel and slag chemical composition are easily obtained by its module and databases [21]. During solidification, variation in solubility of steel dissolved elements that favors inclusion formation are visualized as well [22].

The objective of this work was to evaluate steel cleanliness and reoxidation of modified SAE 1055 steel in industrial production of an electric steel mill. Slag parameters such as binary basicity, CaO/Al_2O_3 ratio, liquid fraction and effective viscosity were correlated with inclusion density to investigate cleanliness after secondary refining. Inclusion population on a rolled bar was compared with results after the secondary refining in order to evaluate reoxidation phenomenon during the continuous casting. Thermodynamic software FactSage and PDF method were used to analyze reoxidation events.

2 MATERIALS AND METHODS

Six heats from steel production in an electric steel mill were selected for this study. Steel grade chosen was a modified SAE 1055, average composition presented in Table 1, manufactured for bearing industry. An ARL 3560 Optical Emission Spectrometer measured steel chemical composition.

Table 1. Average chemical composition (wt.%) of modified SAE 1055.

Steel	C	Si	Mn	P	S*	Al_{total}*	Ca*	N*	T.O.*
SAE 1055	0.555	0.235	0.748	0.013	50	60	1	73	11

** = ppm*

Three different slag compositions were investigated, providing a wider range of chemical composition. Heats A1 and A2 presented a ladle slag in the following oxide system: $CaO\text{-}SiO_2\text{-}MgO\text{-}Al_2O_3\text{-}CaF_2$. A similar slag without the presence of fluoride was used in heats B1, B2, C1 and C2. Binary basicity (B_2) was the key difference between slag B (B_2 = 3.62) and C (B_2 = 1.48). Slags chemical composition were measured by X-ray fluorescence in a Philips PW2600 equipment. A steel and slag samples were withdrawal in the ladle after secondary refining, moments before its release to the continuous casting station. Another steel sample was taken in the end of the process from a rolled bar. This sample also had total oxygen content analyzed by a LECO equipment model TC-436. Figure 1 presents the steelmaking route during the production of modified SAE 1055 and withdrawal points of steel and slag samples.

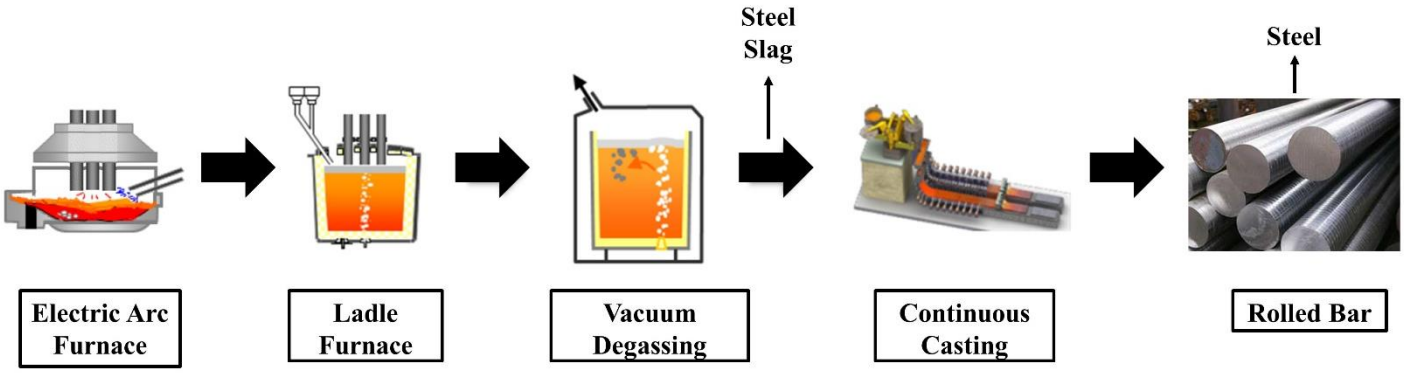

Figure 1. SAE 1055 production route. Steel and slag samples withdrawal points.

Automated SEM/EDS (ASPEX Explorer) equipment provided inclusion data for both steel samples. Steel area analyzed varied from 50 to 100 mm^2. Output data from this equipment included size, diameter and chemical composition of inclusions. They were classified according to specific rules presented in Table 2. Following inclusion types were selected for the present work: spinel, Ca sulfide, CaAl liquid, CaAl mushy, CaAl solid and Silicate.

Table 2. Classification rules used in the present work.

Inclusion Type	Clasification Rule
Spinel	Mg/(Al + Mg + Ca) > 0.1 Al > 30 Ca < 20
Ca Sulfide	Ca > 20 S > 20
CaAl liquid	(Ca + Al) > 50 Al/Ca < 0.8
CaAl mushy	(Ca + Al) > 45 Al/Ca < 1,5
CaAl solid	(Ca + Al) > 45 Al/Ca < 3
Silicate	(Ca + Al + Si) > 50 Si > 5

Thermodynamic software FactSage v7.2 provided data about liquid and solid fraction of slags. *Equilib* module with *FToxid* and *FactPS* databases were used for this

calculation. *Viscosity* module with *Melts* database calculated the viscosity of the liquid fraction of slag. Since metallurgical slags usually have a liquid and a solid fraction, Roscoe-Einstein [23] model, Equation 1, was applied to obtain the effective viscosities of the slags. η_e = effective viscosity; η = liquid viscosity; c = solid fraction.

$$\eta_e = \eta(1 - c)^{-2,5} \quad (1)$$

Where:
- η_e = effective viscosity;
- η = liquid viscosity;
- c = solid fraction.

Equilib module with *FSstel*, *FToxid* and *FactPS* databases calculated inclusions formed during solidification. Temperature was varied from 1600 to 1200 °C and spinel phase was evaluated during solidification. Once steel chemical composition measurement method did not provide dissolved Mg content, a previous step was done to obtain this information. Steel and slag chemical composition after the secondary refining were set in equilibrium using FactSage, providing a dissolved Mg content that was used further for solidification calculation.
Another tool applied to evaluate the formation of spinel inclusion and their relation with reoxidation was the Population Density Function (PDF). This analysis was applied to spinel inclusions present in the rolled bar. Methodology used by Zinngrebe *et al*. [17] and VanEnde *et al*. [18] was replicated. A bin value of 1 was used to organize inclusions by equivalent diameter. Therefore, inclusions were separated and grouped for each range of 1 µm to provide a point as output result of PDF method.

3 RESULTS AND DISCUSSION

3.1 Steel, Slag and Inclusions after Secondary Refining

Steel samples after secondary refining presented similar values on all conditions analyzed. Table 3 summarizes the values of steel chemical composition.

Table 3. Steel chemical composition (wt.%) for samples taken after secondary refining.

Heat	C	Si	Mn	Al_{total}*	S*	Ca*	N*
A1	0.524	0.229	0.797	60	10	12	33
A2	0.551	0.229	0.726	70	20	1	41
B1	0.535	0.239	0.722	80	10	4	36
B2	0.550	0.256	0.756	40	30	8	86
C1	0.533	0.199	0.742	20	110	1	57
C2	0.557	0.268	0.683	30	60	1	79

** = ppm*

In general, they present a good approach to standard composition aimed. Lowest Al_{total} and highest S content visualized for heats C1 and C2 could be a consequence of its chemical composition with an average binary basicity of 1.48. After chemical composition, inclusion population was investigated. Inclusions were classified and the density of each type was calculated. Figure 2 summarizes these results.

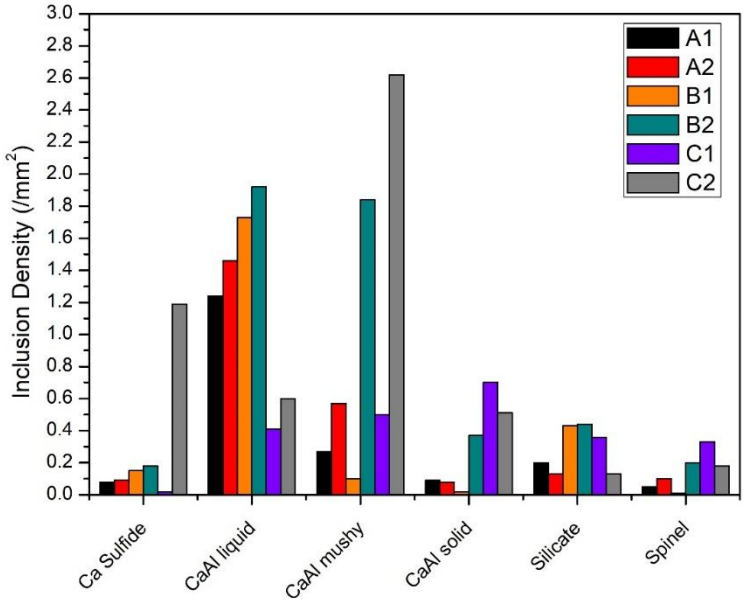

Figure 2. Inclusion density for each type of inclusion after secondary refining.

Ca sulfide had the lowest values among all types, except heat C2. Heats C1 and C2, due to their increased S content could favor the formation of sulfides. At this stage of the process, only heat C2 confirms this anticipation. CaAl liquid was the main type of inclusion found in heats A1, A2, B1 and B2. Slag chemical composition used in these heats with CaO/Al_2O_3 (C/A) ratio below 3 could explain this behavior. Heats C1 and C2 with a C/A above 4 appeared to favor the presence of CaAl inclusions as mushy and solid. CaO/Al_2O_3 ratio has been used as an interesting parameter to evaluate steel cleanliness, with insightful results depending on steel grade and type of inclusions to be removed [24,25]. Silicate inclusions presented similar values for all heats, with slag chemical composition influence diminished. At this stage of the process, formation of spinel is controlled and for all slag practices, their inclusion density is below 0.4 mm^{-2}. Comparing inclusions after secondary refining and at rolled bar would bring comprehensions about which type of inclusion is the main reoxidation product. Subsequently, average inclusion density of all inclusion and standard deviation of each group were evaluated and presented in Figure 3.

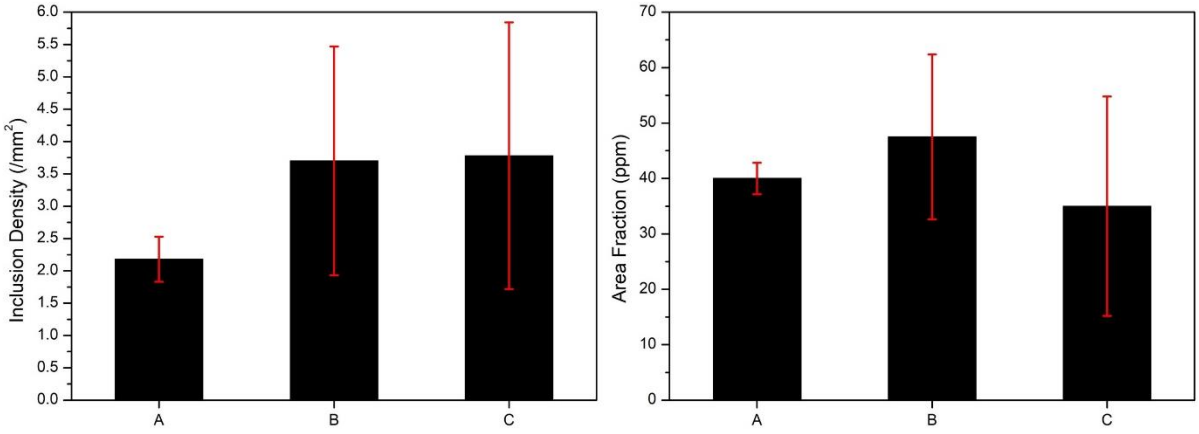

Figure 3. Average inclusion density, average area fraction and standard deviation for each slag practice.

Heats A1 and A2 had the lowest inclusion density and standard deviation at this stage of the process. Heats B1, B2, C1 and C2 had similar inclusion density and an increased standard deviation. From Figure 3, slags with the presence of fluoride (CaF_2) provided a better removal of inclusion during secondary refining. Area fraction results had different pattern than inclusion density. Heats C1 and C2 presented the lower area fraction and B1 and B2 the highest. Slag with fluoride still presents a good result, especially with a lower standard deviation among the heats analyzed. However, one more step is necessary until the solidification of steel. During the continuous casting, reoxidation events could occur resulting in the formation and/or modification of inclusions [9,10]. Thus, analysis of inclusions after this stage becomes an interesting tool to evaluate reoxidation events at continuous casting. Slag samples were collected after secondary refining and their chemical composition is presented in Table 4.

Table 4. Slag chemical composition (wt.%) after secondary refining.

Heat	CaO	SiO_2	MgO	Al_2O_3	FeO	MnO	CaF_2
A1	52.65	15.05	7.49	18.35	0.81	0.23	5.42
A2	55.89	14.97	7.95	17.78	0.82	0.20	2.40
B1	53.26	16.69	9.73	19.37	0.76	0.19	-
B2	51.08	18.27	10.70	18.84	0.85	0.25	-
C1	41.86	29.14	17.85	9.88	0.67	0.60	-
C2	42.70	28.09	18.29	10.02	0.60	0.31	-

The main difference between heats A and B is the presence of fluoride in chemical composition of A1 and A2 slag samples. Furthermore, a slight increase in MgO content is verified on heats B1 and B2. This behavior was expected since the presence of fluoride is capable to reduce MgO saturation point of slags [26]. Among three slag practices, heats C1 and C2 presented the highest SiO_2 and the lowest Al_2O_3 content. This combination of compositions provides a slag with a low binary basicity (1.48) and high C/A ratio (4.25). The sum of FeO and MnO content is controlled below 1.5, obtaining a slag with low oxidation capability. Slag parameters such as binary basicity (B_2), C/A, liquid fraction and effective viscosity were evaluated regarding their influence in steel cleanliness after secondary refining. Table 5 presents these results for all slags analyzed.

Table 5. Binary basicity, CaO/Al_2O_3 ratio, liquid fraction and effective viscosity of slags after secondary refining.

Heat	Binary Basicity	CaO/Al_2O_3	Liquid Fraction (%)	Effective Viscosity (Pa.s)
A1	3.50	2.87	98.32	0.065
A2	3.73	3.14	92.80	0.084
B1	3.19	2.75	95.57	0.091
B2	2.80	2.71	95.54	0.095
C1	1.44	4.24	94.19	0.114
C2	1.52	4.26	88.38	0.132

Binary basicity increased and C/A decreased from heats C to A. All slag presented similar liquid fraction with values above 90 % (except C2 – 88.38%). Nevertheless, effective viscosity was different, being influenced by slag chemical composition. Lowest values found in heats A1 and A2 are explained by the presence of CaF_2,

which is known as a strong flux compound [8,26]. Heats B1 and B2 had an increase in effective viscosity and C1 and C2 presented the highest values. This behavior could be explained by the high values of SiO_2 (~30%) in initial slag composition. An increase in this oxide on liquid fraction of slag leads to an increase of liquid viscosity and subsequently an increase in effective viscosity [27,28]. Correlations between inclusion density and slag parameters shown remarkable results regarding the removal of inclusions. Control of these parameters could provide improvement in steel cleanliness after secondary refining. Figure 4 presents the correlation between parameters in Table 5 and total inclusion density measured for each heat. Results obtained by Reis *et al.* [3] in this same electric steel mill were also plotted to provide a wider range of points and a better visualization of tendency.

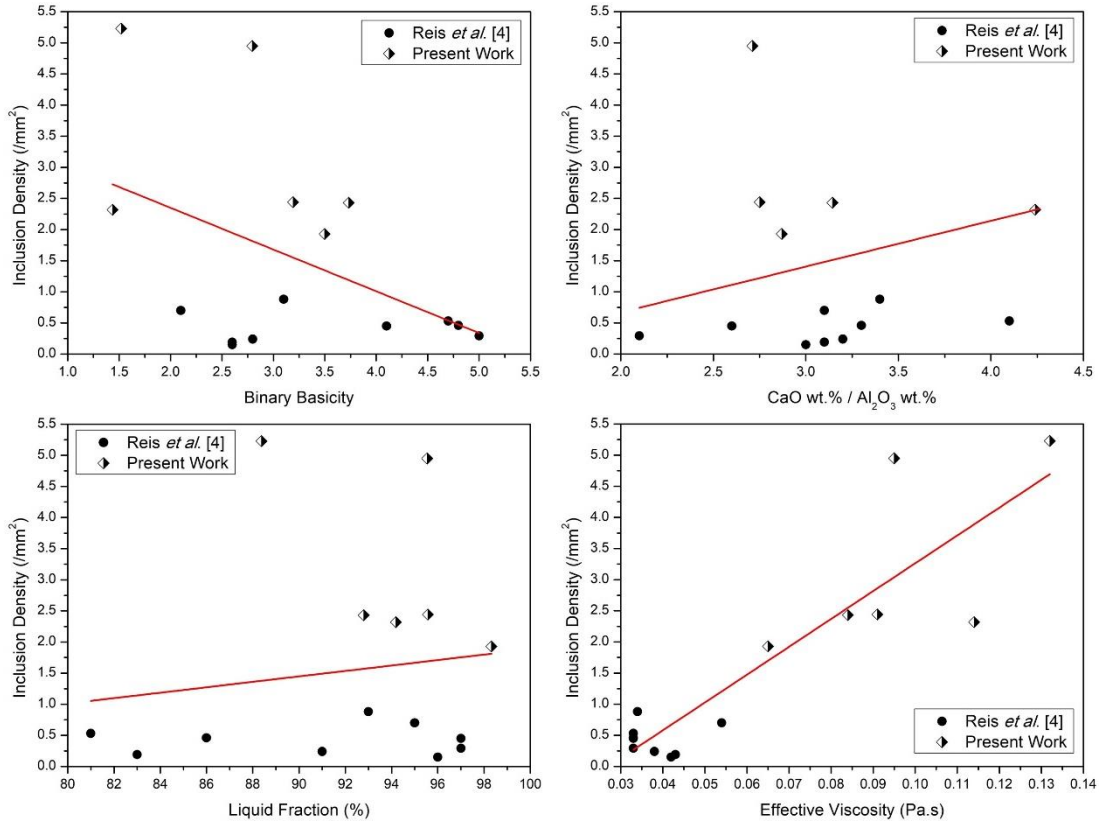

Figure 4. Correlation of inclusion density with binary basicity, CaO/Al_2O_3 ratio, liquid fraction and effective viscosity of slags.

Binary basicity presents a tendency of decrease inclusion density at higher values (3-4). CaO/Al_2O_3 ratio shown lowest values of inclusion density below 3.5 Liquid fraction did not show a correlation with inclusion density. Effective viscosity had the better correlation with inclusion density. An increase in liquid fraction led to a decrease in total inclusion density. This phenomenon corroborates previous statements that claims the liquid fraction of slag to be the part that effective react with steel [3]. Furthermore, an increase in this property also could provide a decrease in the effective viscosity of slags [8]. This behavior is also observed, and the lowest values of effective viscosity are grouped with lowest inclusion density. Remarkable results for this present work were obtained with B_2 above 3, C/A ratio of 3, liquid fraction above 95 % and effective viscosity below 0.100 Pa.s.

3.2 Steel and Inclusions after Rolling Process

Next step was the analyses of steel composition and inclusion population in the end of the process. Comparison between these results in the following subtopic would help to clarifies possible reoxidation events during SAE 1055 industrial production. Table 6 summarizes steel chemical composition results at rolled bar. FactSage calculated Magnesium content based on thermodynamic equilibrium.

Table 6. Steel chemical composition (wt.%) for rolled bar samples.

Heat	C	Si	Mn	Al_{total}*	S*	Ca*	N*	T.O*	Mg*,#
A1	0.550	0.220	0.810	60	20	1	46	9	3
A2	0.560	0.220	0.730	60	20	1	47	13	3
B1	0.560	0.230	0.730	60	20	1	78	10	2
B2	0.550	0.260	0.760	60	40	1	99	8	2
C1	0.550	0.220	0.760	60	100	1	84	12	0.5
C2	0.560	0.260	0.700	60	80	1	86	15	0.6

** = ppm; # = calculated by FactSage*

At this point, all samples present similar composition regarding the standard chemical composition of SAE 1055. Al_{total}, which had variation for Slag C, now is stable at 60 ppm for all samples. Sulphur content remains at higher values for Slag C, with samples C1 and C2 presenting 100 and 80 ppm respectively. This result indicates a lower sulfide's capacity for this composition. Average binary basicity of 1.48 visualized for this slag corroborates the hypothesis of a weaker desulphurization during secondary refining due to its low sulfide capacity [29]. All heats had an increase in Nitrogen content, which can be used as an indirect method to evaluate reoxidation [30]. In general, total oxygen remains below 15 ppm for all samples, being an acceptable value for SAE 1055 after the rolling process. High Mg content is visualized for heats A1 and A2, with higher binary basicity among slag analyzed. This pattern was expected and verifies by previous authors [31]. Subsequently, inclusion population was evaluated and Figure 5 summarizes the results.

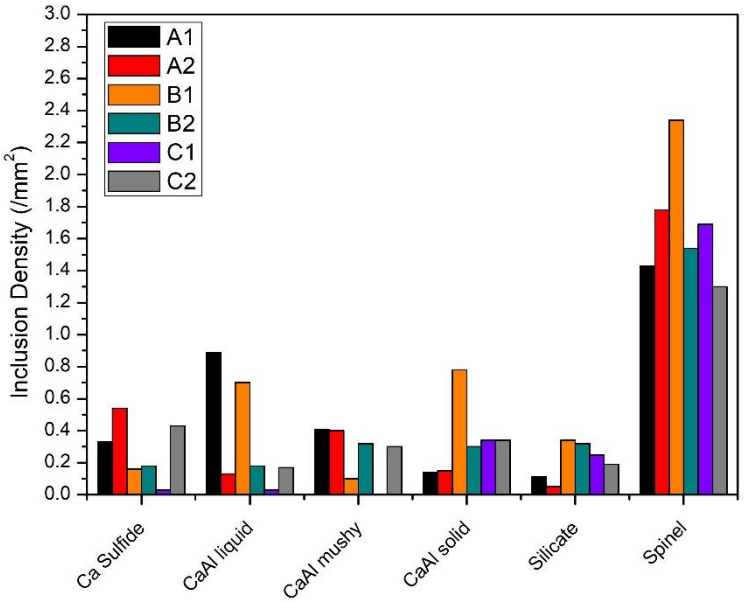

Figure 5. Inclusion density for each type of inclusion at rolled bar.

Spinel inclusions shown an increase compared with samples after secondary refining. Previously, spinel inclusion density was below 0.4 mm^{-2} and now they are

above 1.2 mm^{-2}, with a maximum of almost 2.4 mm^{-2} for heat B1. In general, all heats presented similar behavior regarding the formation of spinel inclusions. Ca sulfide inclusion presented a slight increase, which can be explained by the formation of CaS inclusions during solidification [31]. Even heats C1 and C2, with higher Sulphur values, did not present greater formation of this type of inclusions, with a behavior similar to other slags compositions. CaAl liquid and CaAl mushy diminished at rolled bar, being removed during continuous casting. Tundish slag and mold flux could be responsible to perform the removal of these inclusions. CaAl solid and silicate inclusions did not show greater variation from secondary refining to rolled bar. Results for total inclusion density are represented in Figure 6.

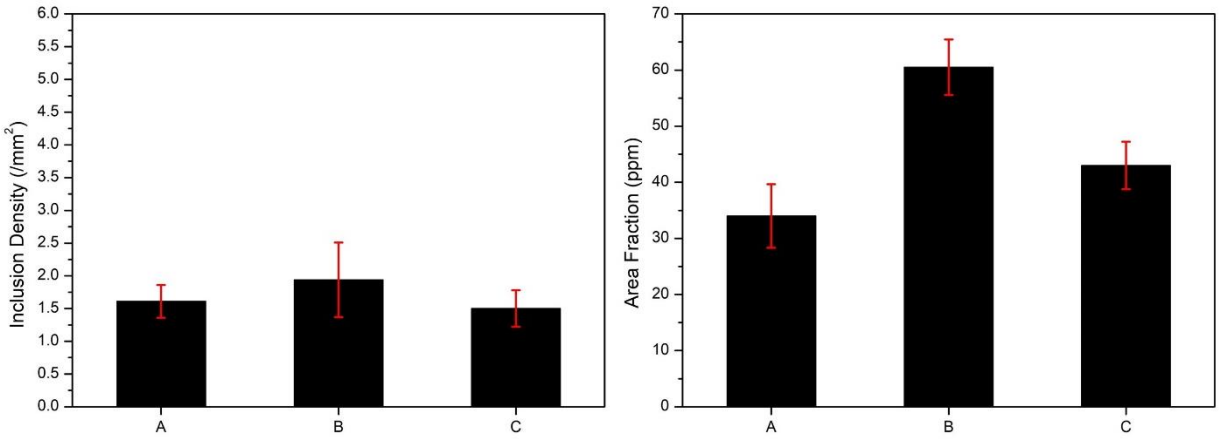

Figure 6. Average inclusion density at rolled bar and standard deviation for each slag practice.

Despite the formation of spinel inclusions as reoxidation products, average inclusion density decreased for all slag practices. Area fraction did not shown great variation compared with samples after secondary refining. Considering that inclusion density decreased, coalesce of inclusion and formation of new inclusion by reoxidation should take control at this part of the process. This represents that once spinel formation would be controlled, SAE 1055 could present a higher steel cleanliness at the end of steelmaking process.

3.3 Reoxidation Evaluation

First analysis regarding the formation of spinel as reoxidation product took in consideration the variation of Nitrogen between the rolled bar and ladle furnace samples. Figure 7 exposes in a graphic form this analysis.

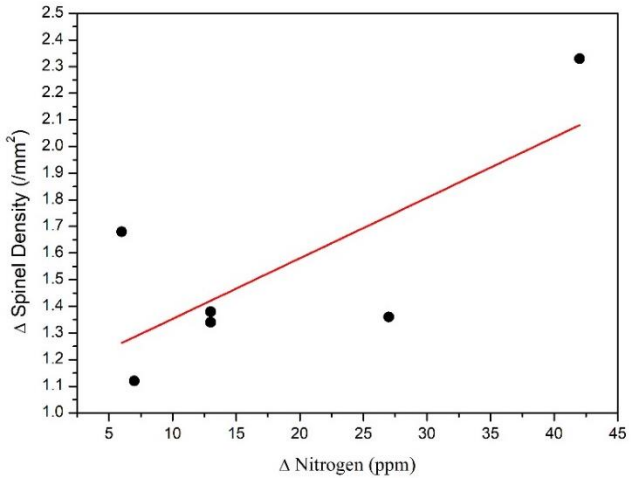

Figure 7. Correlation between nitrogen and spinel density variation between rolled bar (RB) and ladle furnace (LF).

Figure 7 compare the variation (Δ) in spinel inclusion density between the rolled bar and after secondary refining. It is seen a tendency that the increase of spinel inclusion density is correlated with an increase in Nitrogen pick-up. This result reasonably correlates a possible reoxidation product (spinel) with Nitrogen absorption. Another explanation for the formation of spinel inclusions is the decrease of temperature during the solidification. This phenomenon affects the solubility of dissolved elements in steel, favoring the formation of new inclusions [32]. FactSage calculated the formation of spinel inclusion due to the reduction of temperature and the results are presented in Figure 8.

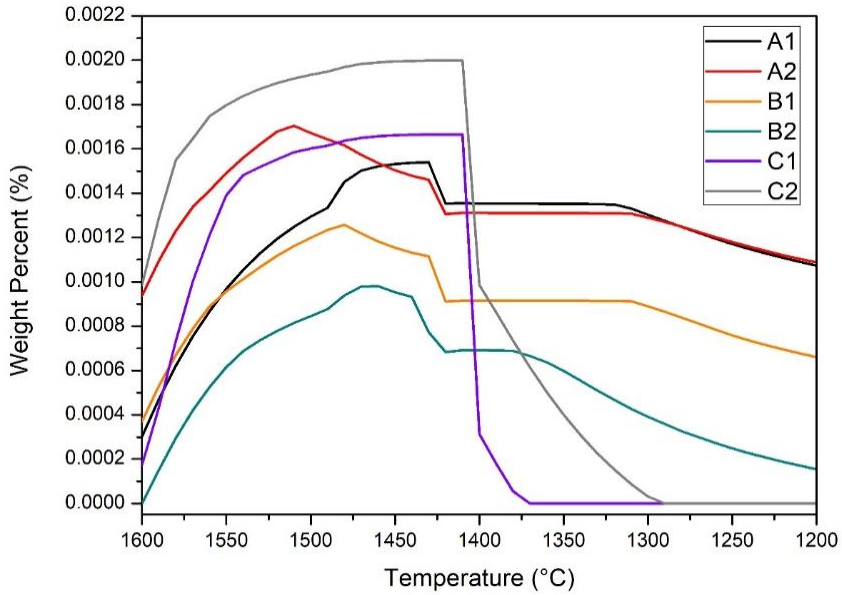

Figure 8. Formation of spinel inclusions due to the decrease of temperature during solidification.

This calculation revealed the formation of spinel phase during solidification process. Heats B1 and B2 shown the smaller formation of spinel phase. In the other hand, A2,C1 and C2 heats had the greatest peak during solidification process. Heats C1 and C2 present a great decrease around 1400 °C. Since Figure 9 presents spinel inclusions as weight percent, at 1400 °C formation of sulfides greatly increases, lowering spinel phase weight percent. Other heats also present formation of sulfides around 1400 °C. Nevertheless, for heats A1, A2, B1 and B2, this formation is less

pronounced, causing a lower decrease in spinel weight percent below 1400 °C. Lastly, spinel inclusions were analyzed using PDF method and results are visualized in Figure 9.

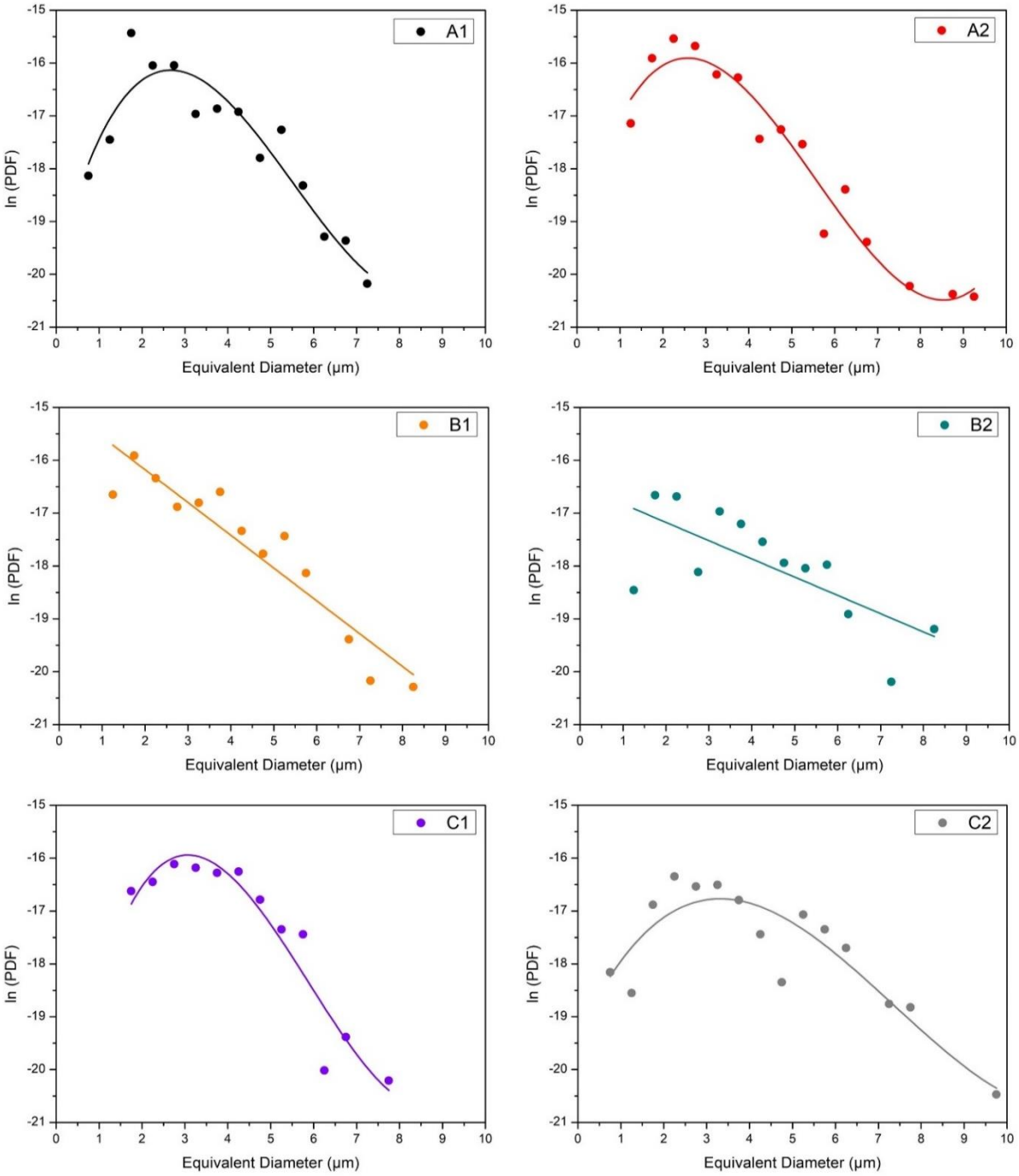

Figure 9. PDF method applied for spinel inclusion observed at rolled bar samples.

Heats A1, A2, C1 and C2 present a lognormal shape, which characterize inclusions formed by reoxidation [17,18]. Reoxidation in these heats could be due to interaction with tundish and mold materials. Gunning mass used in this industry revealed in previous study formation of spinel inclusions after interacts with a similar modified SAE 1005 under laboratorial condition [13]. This could be an explanation for reoxidation events observed in these heats. Differently, a linear fit is observed for heats B1 and B2, indicating that spinel inclusions were not formed due to reoxidation [17,18]. In this case, other inclusions could be modified to spinel and a deeper

investigation is recommended. PDF method surge as an efficient tool to evaluate reoxidation, being used frequently in the past years to clarify this phenomenon [17-19].

4 CONCLUSIONS

The following conclusion were achieved after the evaluation of cleanliness and reoxidation on modified SAE 1055 steel.

- After secondary refining the main type of inclusions found were calcium aluminates. At the rolled bar occurred a decreased in these inclusions and spinel were formed during continuous casting stage.
- Nitrogen variation presents a good correlation with the increase of spinel inclusion at rolled bar, being an efficient indirect method to evaluate reoxidation.
- During solidification, FactSage verified the formation of spinel inclusion with the decrease of temperature for all slags analyzed.
- PDF method clarified formation of spinel after secondary refining. Heats A1, A2, C1 and C2 had spinel formed by reoxidation. For heats B1 and B2, other type of inclusions present after secondary refining was modified to spinel during continuous cast process.
- Slag in $CaO\text{-}SiO_2\text{-}MgO\text{-}Al_2O_3$ system with B_2 and C/A ratio of 3 and 2.7 present better results regarding reoxidation. Control of tundish and mold materials that could modified previous inclusions to spinel would deliver a SAE 1055 with a high steel cleanliness.

Acknowledgements

The authors are thankful for financial support provided by Fundação Luiz Englert (FLE), Coordination for the Improvement of Higher Education Personnel (CAPES) and National Council for Scientific and Technological Development (CNPq).

REFERENCES

1 Pretorius EB, Oltmann HG, Schart BT. An Overview of Steel Cleanliness from an Industry Perspective. AISTech 2013 Proceedings. 2013. 993–1026.
2 Holappa L. Recent Achievements in Iron and Steel Technology. Journal of Chemical Technology and Metallurgy. 2017;52(2): 159-167.
3 Holappa LEK, Helle AS. Inclusion Control in High-Performance Steels. Journal of Materials Processing Tech. 1995;53(1–2):177–186.
4 Reis BH, Bielefeldt WV, Vilela ACF. Efficiency of Inclusion Absorption by Slags during Secondary Refining of Steel. ISIJ International. 2014;54(7):1584–1591.
5 Zhang LF, Thomas BG. State of the Art in Evaluation and Control of Steel Cleanliness. ISIJ International. 2003;43(3):271–291.
6 Holappa L, Nurmi S, Louhenkilpi S. Role of slags in steel refining: is it really understood and fully exploited? La Revue de Métallurgie. 2009;106(1):9-20.
7 Jiang M, Wang XH, Wang WJ. Study on refining slags targeting high cleanliness and lower melting temperature inclusions in Al killed steel. Ironmaking & Steelmaking. 2012;39(1):20–25.
8 Rocha VC, Pereira JAM, Yoshioka A, Bielefeldt WV, Vilela ACF. Evaluation of Secondary Steelmaking Slags and Their Relation with Steel Cleanliness. Metallurgical and Materials Transactions B: Process Metallurgy and Materials Processing Science. 2017;48(June):1423–1432.
9 Hollapa L, Kekkonen M, Louhenkilpi S, Hagemann R, Schröder C, Scheller P. Active Tundish Slag. Steel Research International. 2013;84(7):638-648.
10 Sahai Y. Tundish Technology for Casting Clean Steel A Review. Metallurgical and Materials Transactions B: Process Metallurgy and Materials Processing Science. 2016;47(August):2095-2106.

11 Yan P, Arnout S, Van Ende MA, Zinngrebe E, Jones T, Blanpain B, et al. Steel Reoxidation by Gunning Mass and Tundish Slag. Metallurgical and Materials Transactions B: Process Metallurgy and Materials Processing Science. 2015;46(3):1242–1251.

12 Kekkonen M, Leuverink D, Holappa L. Improving Cleanliness of 16MnCrS5 Case Hardening. Steel Research International. 2017;88(7):1600364.

13 Alves PC, Pereira JAM, Rocha VC, Bielefeldt WV, Vilela ACF. Laboratorial Analysis of Inclusions Formed by Reoxidation in Tundish Steelmaking. Steel Research International. 2018; 89(11):1800248.

14 Michelic SK, Wieser G, Bernhard C. On the Representativeness of Automated SEM/EDS Analyses for Inclusion Characterisation with Special Regard to the Measured Sample Area. ISIJ International. 2011;51(5):769-775.

15 Bartosiaki BG, Pereira JAM, Bielefeldt WV, Vilela ACF. Assessment of inclusion analysis via manual and automated SEM and total oxygen content of steel. Journal of Materials Research and Technology. 2015;4(3):235–240.

16 Tang D, Ferreira ME, Pistorius PC. Automated Inclusion Microanalysis in Steel by Computer-Based Scanning Electron Microscopy: Accelerating Voltage, Backscattered Electron Image Quality, and Analysis Time. Microscopy and Microanalysis. 2017;23(6):1082-1090.

17 Zinngrebe E, Van Hoek C, Visser H, Westendorp A, Jung IH. Inclusion Population Evolution in Ti-alloyed Al-killed Steel during Secondary Steelmaking Process. ISIJ International. 2012;52(1):52-61.

18 Van Ende MA, Guo M, Zinngrebe E, Blanpain B, Jung IH. Evolution of Non-Metallic Inclusions in Secondary Steelmaking Learning from Inclusion Size Distributions. ISIJ International. 2013;53(11):1974-1982.

19 Adaba O, Kaushik P, O'Malley RJ, Lekakh SN, Richards VL, Mantel E, Hall R, Ellis EJ. Characteristics of Spinel Inclusions formed after Reoxidation of Calcium Treated Aluminum Killed Steel. AISTech 2016 Proceedings. 2016. 2559-2572.

20 Choudhary SK, Ghosh A. Mathematical Model for Prediction of Composition of Inclusions Formed during Solidification of Liquid Steel. ISIJ International. 2009;49(12):1819-1827.

21 Bale CW, Bélisle E Chartrand P, Decterov SA, Eriksson G, Gheribi AE, Hack K, Jung IH, Kang YB, Melançon J, Pelton AD, Petersen S, Robelin C, Sangster J, Spencer P, Van Ende MA. FactSage thermochemical software and databases, 2010–2016. CALPHAD. 2016;54(December):35-53.

22 You D, Michelic SK, Presoly P, Liu J, Bernhard C. Modeling Inclusion Formation during Solidification of Steel. Metals. 2017;7(11):460.

23 Roscoe R. The viscosity of suspensions of rigid spheres. British Journal of Applied Physics. 1952;3(8):267-269.

24 Harada A, Matsui A, Nabeshima S, Kikuchi N, Miki Y. Effect of Slag Composition on $MgO{\cdot}Al_2O_3$ Spinel-Type Inclusions in Molten Steel. ISIJ International. 2017;57(9):1546-1552.

25 Ji Y, Liu C, Lu Y, Yu H. Effects of FeO and CaO/Al_2O_3 Ratio in Slag on the Cleanliness of Al-Killed Steel. Metallurgical and Materials Transactions B: Process Metallurgy and Materials Processing Science. 2018;49(December):3127-3136.

26 Pretorius EB. The Effect of Fluorspar in Steelmaking Slags. [acesso em 10 junho 2019]. Disponível em: http://etech.lwbref.com/Downloads/Theory/The%20Effect%20of%20Fluorspar%20in%20Steelmaking%20Slags.pdf.

27 Kim TS, Park JH. Structure-Viscosity Relationship of Low-silica Calcium Aluminosilicate Melts. ISIJ International. 2014;54(9):2031-2038

28 Kim TS, Heo JH, Kang JG, Han JS, Park JY. Understanding Viscosity-Structure Relationship of Slags and Its Influence on Metallurgical Processes. Proceedings of the First Global Conference on Extractive Metallurgy. 2018. 1121-1127

29 Nzotta MM, Sichen D, Seetharaman. A Study Of The Sulfide Capacities of Iron-Oxide Containing Slags. Metallurgical and Materials Transactions B: Process Metallurgy and Materials Processing Science. 1999;30(October):909-920.

30 Zhang L. Indirect Methods of Detecting and Evaluating Inclusions in Steel—A Review. Journal of Iron and Steel Research, International. 2006;13(4):1-8.

31 Bartosiaki BG, Pereira JAM, Bielefeldt WV, Vilela ACF. Estudo de Inclusões Não-Metálicas em Aços Durante Tratamento em Desgaseificador a Vácuo e Início do Lingotamento Contínuo. Anais do 45° Seminário de Aciaria – Internacional. 2014. 471-480.

32 Gui L, Long M, Huang Y, Chen D, Chen H, Duan H, Yu S. Effects of Inclusion Precipitation, Partition Coefficient, and Phase Transition on Microsegregation for High-Sulfur Steel Solidification. Metallurgical and Materials Transactions B: Process Metallurgy and Materials Processing Science. 2018;49(December):3280-3292.